Engineered *Bacillus subtilis* as oral probiotics to target circulating lactic acid

Mengdi Yang[1], Noah Hutchinson[3], Jianing Yin[1], Ming Guan[1], Zongqi Wang[3], Peiru Chen[2], Shaobo Yang[1], Justin D. Crane[4], Ke Zhang[1,2], Jiahe Li[3]*

[1]Department of Bioengineering, Northeastern University, Boston, MA, 02115, United States.

[2]Department of Chemistry, Northeastern University, Boston, MA, 02115, United States.

[3]Department of Biomedical Engineering, University of Michigan, Ann Arbor, MI, 48109, United States.

[4]Internal Medicine Research Unit, Pfizer Inc., 1 Portland Street, Cambridge, MA 02139

*Correspondence: Jiahe Li, Department of Biomedical Engineering, University of Michigan, Ann Arbor, MI, 48109, United States. Email: jiaheli@med.umich.edu.

Abstract

Lactic acid or lactate, a key byproduct of anaerobic glycolysis, plays pivotal roles in routine metabolism. An increase in lactic acid is observed in various pathological conditions such as cancer, diabetes, genetic mitochondrial disease, and aging. While several groups have proposed small molecule inhibitors to reduce circulating lactic acid, there are few clinically relevant ways to manage acute or chronic elevations in lactic acid in patients. In addition, recent evidence suggests that lactic acid exchanges between the gut, blood, and peripheral tissues, and professional marathon runners harbor specific gut microbial species that more efficiently metabolize lactic acid. Inspired by these findings, this work sought to engineer probiotic *B. subtilis* strains to express lactate oxidase that could increase circulating lactic acid catabolism after delivery to the gut. After optimization, oral administration of engineered *B. subtilis* to the gut of mice reduced the elevation in blood lactic acid levels after exogenous lactic acid challenge without affecting normal gut microbiota composition, inflammation or liver enzymes. Taken together, through the oral delivery of engineered probiotics to the gastrointestinal tract, our proof-of-concept study offers a new opportunity to therapeutically target diseases where blood lactic acid is elevated, and provides a new approach to “knocking down” metabolites to help understand the roles of metabolites in host physiological and pathological processes.

Introduction

Lactate is a hydroxycarboxylic acid produced from glucose during anaerobic glycolysis which is formed when glucose in the cytosol converts into pyruvate, catalyzed by L-lactate dehydrogenase (LDH)[1]. As a central product of anaerobic glycolysis, L-lactate serves as a key biomarker for assessing human physiological conditions, including cancer, diabetes, and obesity[1, 2]. Maintaining L-lactate homeostasis is crucial for various physiological processes, such as energy regulation, redox homeostasis, and the control of fatty acid metabolism[1]. The accumulation of lactate can lead to lactic acidosis, which is associated with increased mortality[3]. Studies have revealed that elevated lactate levels can activate inflammatory responses in different organs[4], hinder wound healing[5], and contribute to cancer development[6]. Furthermore, imbalances in L-lactate also affect the maintenance of long-term memory formation and cognitive function[7]. Given these implications, it is essential to manage healthy L-lactate levels. Various treatment methods have been developed, including oxygen therapy[8], intravenous fluid replenishment[9], medications targeting LDH[10] or lactate transporters[11], and addressing associated symptoms or organ dysfunctions. However, these methods do not directly target lactate itself, are often expensive, and require specific environments, limiting their widespread use.

Recently, a new strategy was developed to mitigate lactate upregulation by utilizing a dual-enzyme system called "LOXCAT"[12]. This system can convert extracellular lactate and oxygen to pyruvate and water through two enzymes (Fig. 1A). The first enzyme is lactate oxidase (LOX), which is used by bacteria, yeasts, and fungi to efficiently converts lactate and oxygen to pyruvate and H_2O_2. However, the drawback of this oxidation process is the generation of a cytotoxic product, hydrogen peroxide. To address this, the second enzyme, *Escherichia coli* catalase (CAT), is genetically fused with LOX rapidly to break down H_2O_2 into harmless water and oxygen. This enzyme delivery strategy concurrently tackles the elevation of serum lactate and reductive stress by directly targeting lactate. However, the direct injection of bacterial enzymes into the bloodstream faces challenges for translation: (1) The LOXCAT fusion enzymes, derived from bacteria, may trigger protective immune responses to produce neutralizing antibodies[13]; (2) enzymes are susceptible to protease degradation in the bloodstream; (3) the LOXCAT fusion enzymes have short serum half-lives[12], necessitating repeated injections to maintain a lasting therapeutic effect, (4) enzyme replacement therapies can be very costly and (5) biologics generally require proper storage conditions to extend the shelf life. To address these limitations, we propose to engineer *Bacillus subtilis* (*B. subtilis*) to express recombinant enzymes, which will enable the oral supplementation of LOXCAT-expressing bacteria as probiotics to modulate the systemic lactate levels (Fig. 1B). This strategy is based on evidence that lactic acid can freely

move between the gut lumen, circulation, and peripheral tissues[14-16] and the finding that professional marathon runners have enriched gut commensal bacteria responsible for more efficient catabolism of lactic acid[16]. The study on the microbiome of marathon runners provides another link between activities of gut microbes and blood lactic acid levels in the host. While isolating and providing these special lactic acid-modulating commensal bacteria could be an option to target systemic lactic acid, a probiotics-based system can provide a more attractive platform amenable to genetic engineering with existing synthetic biology tools. Moreover, engineered probiotics can become a generalized and translatable platform due to the safety and compliance in comparison to identifying commensal bacteria with special traits from a subset of healthy donors. Importantly, we focus on *B. subtilis* because it not only meets generally recognized as safe (GRAS) standards set by the Food and Drug Administration (FDA)[17], but also can form spores to survive in extreme environments such as acidic pH and harsh gastric conditions[18]. These characteristics have been harnessed to prolong the shelf-life and thermostability of biologics for various applications such as vaccine development and catalyst[19-21].

Results

Genomic integration of lactate oxidase and catalase in multiple *B. subtilis* strains

B. subtilis is a Gram-positive, rod-shaped, endospore-forming bacterium isolated from soil, widely utilized for heterologous protein production[21]. This study focuses on *B. subtilis* for several reasons. Firstly, *B. subtilis* has a long track record of safety and efficacy in human probiotic supplements [17]. Secondly, its well-established annotated genomic information, physiological data, and easy genetic manipulation make *B. subtilis* an ideal microbe candidate for therapeutic engineering[22]. Thirdly, engineered *B. subtilis* can be manufactured into spores that provide recombinant proteins with high thermostability and a long shelf life[18]. Several clinical studies have confirmed that *B. subtilis* spores can germinate in the human and animal small intestine[18, 23], providing possibilities for feeding spores to improve treatment efficacy. Of note, *B. subtilis* strain has been engineered by others to constitutively expresses an acetaldehyde dehydrogenase enzyme to prevent toxic accumulation of aldehydes from alcohol consumption[24].

Motivated by our earlier effort in developing a *B. subtilis* expression platform for direct secretion of nanobodies[20], we initially attempted to produce recombinant enzymes extracellularly by employing the Sec-dependent secretion pathway via fusion with a signal peptide (*amyQ*) in *B.*

subtilis WB800N. While WB800N is optimized for extracellular protein production since eight proteases are knocked out, it failed to produce detectable LOX in the supernatant (Fig. S1). It is possible that LOX (~ 41 kDa as a monomer) can undergo tetramerization to form an even larger protein complex that prohibits efficient protein export, which is one limitation of the Sec-dependent protein secretion pathway. Moreover, the *amyQ* secretion signal peptide, reliant on the bacterial Sec pathway, necessitates the unfolding of the secreted protein for translocation through the membrane followed by correct refolding[25]. If LOX cannot refold correctly, it is susceptible to misfolding and degradation. Subsequently, our focus shifted to establishing an intracellular expression system by integrating the target gene into a nonessential locus (*amyE*) in the chromosome through homologous recombination[26]. To demonstrate the versatility of our approach, we sought to build and test our constructs in four different *B. subtilis* strains including PY79, WB800N, NCIB3610, and HU58 that have been employed for various preclinical trials[26-31]. While PY79 and WB800N are amenable to direct transformation, NCIB3610 and HU58 require phage transduction for genetic manipulation. However, we primarily focused on PY79 in this work because this strain (1) is a widely used strain in laboratory studies with the whole genome sequenced, (2) lacks many mobile genetic elements found in other *B. subtilis* strains that may confer antibiotic resistance through horizontal gene transfer, (3) has proven safe to vertebrates (e.g., rats, mice, and chickens), and (4) has been genetically modified with specific traits for *in vivo* applications[30, 32-36]. Importantly, PY79 has been repurposed as probiotics to remove toxic byproducts from alcohol consumption[24].

To enable high-level expression of transgenes from a single copy in the genome, we chose a highly active promoter termed $P_{NBP3510}$ as the initial component of the construction[37]. All integration fragments targeting the *amyE* locus consist of three essential components: the *amyE* 5' homologous arm fused with the $P_{NBP3510}$, the gene of interest (GOI), and the *amyE* 3' homologous arm coupled with a chloramphenicol resistance selection marker (Fig. 1C). In pursuit of optimal catalase activity, which is necessary to break down cytotoxic hydrogen peroxide derived from LOX activity, we selected a homologous catalase from *Ureibacillus thermosphaericus*, UtCAT, which has been shown to be more active and stable than the *E. coli* CAT[38]. Various combinations were then created using LOX, UtCAT, and CAT (Fig 1D). To couple the expression of UtCAT or CAT with LOX in a single gene cassette, we explored two different configurations. The first strategy is to construct a synthetic operon consisting of the $P_{NBP2510}$ promoter with two separate ribosome binding sequences to drive the expression of LOX and UtCAT or CAT, respectively. Two strong RBSs (R0 and B0035), tailored for *B. subtilis* and *E.coli*,

were found to be equally active in *B. subtilis* strains. Consequently, we generated *ΔamyE::cat*_LOX, *ΔamyE::cat*_LOX_B0035_UtCAT, and *ΔamyE::cat*_LOX_R0_UtCAT strains. In addition to the operon configuration, we also generated fusion proteins, where we inserted a linker peptide (L20) between CAT (UtCAT) and LOX, which was previously designed for intravenous administration of LOXCAT[12]. The expression of all constructs was confirmed through Western Blot analysis (Fig. S2). Finally, we constructed the integration fragment incorporating the super-folding green fluorescent protein (sfGFP) as a control which lacks the ability to catabolize lactate, thereby serving as a bacterial load mimic without affecting lactate metabolism[16].

Engineered *B. subtilis* exhibited catalase and lactate oxidase activities as whole cell biocatalysts

The activity of catalase in the CAT and UtCAT strains can be ascertained by monitoring the amount of oxygen gas generated after direct incubation of engineered strains with 3% hydrogen peroxide. By adapting a previous method[39], O_2 were trapped by the foam in aqueous buffer containing a surfactant, Triton-X100 inside the test tubes, and the height of the foam in the geometrically confined tubes correlated with the degrees of reactions and catalase activities. Interestingly, we observed that LOX and sfGFP alone exhibited the ability to break down H_2O_2, and the efficiencies were comparable to those strains expressing the CAT or UtCAT transgenes from the *amyE* locus (Fig. 2A). This may be due to the inherent ability of *B. subtilis* vegetative cells to constitutively secrete KatA, which confers resistance to oxidative stress[40]. The CAT or UtCAT constructs showed only a marginal improvement in breaking down H_2O_2 compared to sfGFP and LOX alone suggesting that the endogenous catalase activities of *B. subtilis* were sufficient to degrade H_2O_2, a toxic product of LOX, without the need to co-express recombinant CAT or UtCAT. However, it's noteworthy that the endogenous and recombinant catalase activities varied among different *B. subtilis* derived strains. For instance, no significant improvement of catalase activities was observed in NCIB3610 strains that were engineered to overexpress UtCAT or CAT through either a synthetic operon or a genetic fusion configuration, in comparison to those expressing only LOX or sfGFP (Fig. S3A). Conversely, in WB800N, recombinant CAT or UTCAT enhanced catalase activities compared to LOX or sfGFP alone (Fig. S3B). In the case of HU58, a human gut-isolated strain[35], a minor increase in catalase activities was observed by expressing UtCAT or CAT (Fig. S3C). Based on the above findings, we reasoned that expressing a single transgene LOX by itself would be sufficient to safely metabolize lactate without an additional copy of catalase in *B. subtilis*. To assess the capacity of this strain to break down extracellular lactate, *B. subtilis* cells were washed, concentrated, and resuspended to OD_{600}= 1 in 1xPBS supplemented with 5

mM Na-L-lactate, simulating a relatively high lactate concentration during lactic acidosis. Notably, PY79 expressing LOX completely removed 5 mM lactate within 1 hour (Fig 2B). Co-expression of LOX with UtCAT or CAT in *B. subtilis* did not enhance the lactate consumption compared to expression of LOX alone (Fig. S4). To demonstrate the versatility of LOX expression in promoting the degradation of lactic acid, we further engineered three additional *B. subtilis* strains (WB800N, NCIB3610, and HU58) to express LOX, which led to complete breakdown of 5 mM lactate within 1-3 hours (Fig. 2C-E). Based on our findings, we concluded that *B. subtilis* strains expressing intracellular LOX can directly serve as a whole cell biocatalyst to break down extracellular lactate without the need to use purified recombinant enzymes.

Oral supplementation of engineered *B. subtilis* to the gut of mice can reduce elevations in blood lactate after exogenous lactate administration

After confirming *B. subtilis* strains expressing LOX can efficiently remove lactate *in vitro*, we sought to assess whether orally administering *B. subtilis* expressing LOX could help mitigate elevated blood lactate. Since the derivatives of PY79 have been repurposed as probiotics to remove toxic byproducts from alcohol consumption[24], we primarily chosen PY79 expressing LOX for our *in vivo* proof-of-concept studies. We attempted to harness spores' superior resistance to extreme conditions as the viability of spores can be minimally affected by the acidic environment in the stomach compared to that of vegetative cells. In the meantime, however, since the strong promoter $P_{NBP3510}$ is only active in vegetative cells, solely administering spores may require additional time for germination into vegetative cells *in vivo* to turn on the expression of LOX. Therefore, to combine the benefits of spore resistance and the strong LOX expression in vegetative cells of *B. subtilis*, we opted to feed mice with a mixture of a combination of a medium dose of 10^8 CFU spores and a high dose of 10^{10} CFU vegetative cells per day. This strategy is supported by a recent study showing that feeding rats up to 10^{11} CFU/kg body weight spores per day for 90 days did not cause clinically significant side effects[30]. Additionally, for vegetative cells, the dosages varied from 10^4 to 10^{10} CFU/ml in the literature [33, 41, 42]. To induce an experimental lactate upregulation, a single bolus subcutaneous injection of 2.3 g per kg of body weight Na-L-lactate was able to transiently increase blood lactate levels (data are not provided), consistent with previous works by others with a similar dose level[43]. After establishing an experimental lactate induction model in mice, 6-8 week-old wild type C57BL/6 mice were randomly assigned to two groups: *B. subtilis*^{LOX} and *B. subtilis*^{sfGFP} (n=10 each), followed by oral gavage with corresponding strains once per day for three consecutive days. The *B. subtilis*^{sfGFP} control lacks the ability to catabolize lactate (Fig. 2B), thereby serving as a bacterial load mimic without

affecting lactate metabolism. On Day 3, 20 minutes after the last oral administration, a subcutaneous injection of 2.3 g/kg body weight Na-L-lactate was administered to induce experimental lactate spike (Fig. 3A). In comparison to *B. subtilis*^{sfGFP}, *B. subtilis*^{LOX} exhibited increases in blood lactate with a lower magnitude (~ 5 mM) than that of the sfGFP control group (~8 mM) at 50-70 minutes after injection (Fig. 3B). To confirm whether the effectiveness of orally administered *B. subtilis*^{LOX} in mitigating systemic lactate spike was not limited to the C57BL/6 strain, we extended the study to another popular mouse strain, CD-1. It was found that the LOX-treated groups consistently led to a lower magnitude of blood lactate spike compared to that of the sfGFP group (Fig. S5). This observation suggests that the impact of engineered *B. subtilis* on blood lactate levels is not specific to a particular mouse model. To understand whether feeding mice with engineered *B. subtilis* strains caused systemic toxicity, plasma or serum samples were collected at 0hr (before oral gavage), 24 hours, 72 hours, and Day 7 after 1st oral gavage for different biochemical assays (Fig. 3C). We found that serum aminotransferase (ALT) and aspartate aminotransferase (AST) levels in both groups were not significantly different from those in the PBS group (Fig. 3D). One mouse in the LOX group exhibited an elevated AST level. However, it is important to note that the observed levels for both ALT and AST are considerably lower than the upper limits of the reference ranges for healthy mouse serum, which are 24.3 - 115.25 U/L for ALT and 39.55 - 386.05 U/L for AST. In parallel, inflammatory cytokine and chemokine levels from plasma were quantified by the Luminex Assay. Compared to the PBS group, *B. subtilis* administration did not elevate representative pro-inflammatory factors including IL-1β and IFNγ. Additionally, the key factor associated with a cytokine storm, monocyte chemoattractant protein 1 (MCP1), exhibited lower levels than the PBS group (Fig. 3E). Anti-inflammatory cytokines (IL-10, IL-12p70) and adaptive immune cytokines (GM-CSF, IL-2, IL-4) were also notably lower than in the PBS group (Fig. S6). Moreover, the concentration of TNFα was extremely low and was undetected in all samples. These findings strongly suggest that feeding *B. subtilis* did not induce any discernible side effects in mice.

Feeding *B. subtilis* PY79 didn't disturb gut microbiome

Subsequently, we assessed whether feeding *B. subtilis* would influence the overall composition of the gut microbiome (Fig. 4A). *B. subtilis* was detected in feces one day after the initial oral gavage and increased with subsequent administrations. However, the total amount of *B. subtilis* reduced at 7 days after the first gavage, likely attributed to the cessation of *B. subtilis* administration and the lack of ability to colonize the mouse gut by probiotics in general. By 15 days after the initial gavage, *B. subtilis* was no longer detectable in fecal samples, indicating that

B. subtilis does not establish long-term colonization in the gut in C57BL/6 mice (Fig. 4B). Similar observations were found in CD-1 mice 18 days after the first gavage (Fig. S7). Furthermore, there were no discernible differences in colonization between the LOX and sfGFP groups, indicating that the expression of enzymes does not significantly impact *B. subtilis* gut colonization. Stool samples were also collected at the designated time points for 16S rRNA analysis. Overall, *B. subtilis* was absent in the top 10 genus-level microbial (Fig. S8). Pairwise Adonis testing of weighted UniFrac distances between treatment groups and the Day 1, 3, and 7 timepoints after the first gavage revealed no difference in β-diversity between the LOX, sfGFP and PBS groups ($p>0.05$) (Fig. 4C). Measures of α-diversity such as Chao1 (Fig. 4D) or Shannon (Fig. S9) revealed no differences between treatment groups ($p=0.488$ and 0.16 for Shannon and Chao1, respectively) or time points ($p=0.137$ and 0.67 for Shannon and Chao1, respectively). This indicates that even at low abundance, engineered *B. subtilis* can introduce the functional impact of LOX on blood lactate levels without significantly altering the microbial community in the host.

Discussion

Lactate balance, often referred to as lactate homeostasis, serves as a crucial indicator for overall metabolic health and clinical diagnosis[44]. One clinical manifestation of dysfunctional lactate metabolism is lactic acidosis, associated with various diseases such as mitochondrial dysfunction, liver disorders, diabetes, and hypoxia, among others[44-46]. In clinical studies, a lactate clearance greater than 20% in the first 8 hours has been linked to a 22% lower risk of death compared to cases with less than 20% clearance[47]. Current clinical treatments for lactic acidosis are predominantly based on treating the symptoms rather than direct lactate targeting. In contrast to these efforts, a recent proof-of-principle study by others demonstrated that directly targeting the common downstream metabolite, lactate, through intravenous administration of recombinant enzymes, markedly reduced disease symptoms in a preclinical mouse model of mitochondrial disease[12]. However, biologic enzyme therapy is expensive and requires frequent administration, as small molecule and enzyme-based drugs face rapid clearance *in vivo*. Additionally, biologics demand proper storage conditions to maintain long shelf life and biological activities.

We sought to address these challenges by integrating LOX catalytic enzymes into *B. subtilis* to target elevated blood lactate from the gut. Importantly, we focus on *B. subtilis* in this work due to its long track record of safety and efficacy in human probiotic supplements, meeting the GRAS standards set by the FDA[17]. Additionally, *B. subtilis* can form spores to survive in extreme environments such as acidic pH and harsh gastric conditions[18], and these characteristics have

been harnessed to prolong the shelf-life and thermostability of biologics in different applications[19, 20]. Prior fundamental studies indicate the frequent exchange of lactic acid between the gastrointestinal tract and the blood. Furthermore, it was found that marathon runners have enriched gut commensal bacteria with more efficient catabolism of lactic acid. These findings suggest the possibility of modulating systemic lactic acid by manipulating its metabolism in the gut. We chose to engineer probiotics because they are more amenable to genetic manipulation benefiting from existing tools in synthetic biology. While we began this work by generating different genetic configurations for comparison in *B. subtilis* strains, we later found that simple expression of LOX itself coupled with the endogenous catalase activities in bacteria could achieve rapid lactate clearance *in vitro*. Furthermore, we demonstrated that orally supplementing mice with a combination of engineered *B. subtilis* spores and vegetative cells expressing LOX can mitigate the lactate spike in mouse models with experimental lactate induction without disrupting the intestinal microbiome community or inducing any observable side effects. We chose *B. subtilis* as our chassis because oral administration of *B. subtilis* has been demonstrated to have positive impacts on human gut health. For example, it enhances function of the host immune system, provides protection against infections, and produces nutrients with high bioavailability[48]. However, our proof-of-concept work opens possibilities for engineering other bacterial chassis for reducing lactate accumulation, presenting an alternative strategy in sports medicine, metabolic disorders, and gut health.

However, there are still some limitations that can be improved in the future. Firstly, the present work employed an experimental lactic acid induction mouse model via a subcutaneous injection of sodium lactate. However, it will be necessary to test more clinically relevant conditions such as treadmill exercise or models of mitochondrial disease to assess the health benefits of *B. subtilis* expressing LOX by conducting a longer treatment time frame. Secondly, since the promoter we employed is only active in the vegetative cells, spore germination is required in the gut to turn on the expression of LOX. However, the vegetative state of *B. subtilis* is less resistant to the acidic gastric conditions. Therefore, to ensure immediate delivery of LOX enzymes *by B. subtilis* while maintaining the viability of *B. subtilis* for sustained delivery in the gastrointestinal tract, we orally gavaged the mice with a mixture of vegetative cells and spores in a defined ratio. Future work may benefit from a comprehensive optimization of different ratios between spores and vegetative cells to achieve a more efficient delivery of LOX-expressing bacteria to the gut. Thirdly, given the data we have presented, the consumption of extracellular lactic acid does not require overexpression of a lactate importer. It remains to be addressed whether lactic acid passively

diffused into engineered *B. subtilis* or is internalized by a native lactate importer[49]. Nevertheless, it is possible to further improve the efficiency of the lactic acid breakdown by co-expressing a lactate to facilitate its uptake. Finally, while we focus on engineering *B. subtilis*, it is attractive to compare *B. subtilis* to other existing bacterial chassis such as *E. coli Nissle* and commensal bacteria to identify an optimized vector for the delivery of LOX enzyme to curtail lactic acid upregulation.

Material and Method

Chemicals and Reagent

All chemicals and bacterial culture broth were purchased from Fisher Scientific International Inc. (Cambridge, MA, USA) unless otherwise noted, and were of the highest purity or analytical grade commercially available. All molecular cloning reagents including restriction enzymes, competent cells, and the HIFI assembly kit were purchased from New England Biolabs (Ipswich, MA, USA). DNA oligonucleotides were ordered from Sigma Aldrich (St. Louis, MO, USA). LOX,CAT, and UtCAT gblock were ordered from IDT with *B. subtilis* codon optimization.

B. subtilis General Growth Conditions

B. subtilis strains were grown at 30°C, 220rpm overnight in LB medium with or without 5ug/ml chloramphenicol. Overnight bacterial culture was diluted 10 times followed by 37°C 220rpm culturing until the OD_{600} reached between 0.6 and 0.8. For *in vivo* studies, bacteria were stored in formulation buffer (2.28g/L KH_2PO_4, 14.5g/L K_2HPO_4, 15% glycerol, pH 7.5) at 10^{11} CFU/ml at -80 °C.

Constitutive Strain Construction

All *B. subtilis* strains were constructed in WB800N first. Primers can be found in Supplementary Table 1. All constructs were confirmed by Sanger sequencing.

All *amyE* locus integration fragments contain three parts: *amyE* 5' arm with $P_{NBP3510}$, GOI, and *amyE* 3' arm with chloramphenicol resistance. The integration fragment was assembled from different plasmids and chromosomal DNA of *B. subtilis* to make *ΔamyE::cat*_sfGFP first which was used as a new template to later make LOX constructs. FLAG and HA tag was added at 3' of

LOX and UtCAT respectively. For fusion enzyme CAT_L20_LOX and UtCAT_L20_LOX, FLAG and HA was added at 5' of CAT and 3' of UtCAT respectively.

*ΔamyE::cat*_sfGFP: The *amyE* 5' arm was amplified through WB800N genomic DNA with the primer B685_V2/B742. $P_{NBP3510}$_sfGFP was amplified from WBSGFP with B741/B747. AmyE 3' arm with was amplified through lab plasmid pHT01-NBP3510-sfGFP with B746/B690. Three fragments were first combined through HIFI assembly kit followed by cementing pcr via B685_V2/B690 before transformation into to *B. subtilis* as described below.

ΔamyE::cat _LOX: *amyE* 5' arm with $P_{NBP3510}$ and with *amyE* 3' arm with Cm^r were amplified by B685_V2/B774 and B776/B690 separately through the chromosomal DNA of PY79 *ΔamyE::cat*_sfGFP. LOX was amplified via B775/B777.

*ΔamyE::cat*_CAT_L20_LOX: *amyE* 5' arm with $P_{NBP3510}$ and *amyE* 3' arm with Cm^r were amplified by B685_V2/B781 and B776/B690 separately through chromosomal DNA of PY79 *ΔamyE::cat*_sfGFP. CAT was amplified via B782/B218 through Gblock. LOX was amplified via B218/B783

*ΔamyE::cat*_LOX_B0035_UtCAT: *amyE* 5' arm with LOX was amplified via B685_V2/B614 through chromosomal DNA of PY79 *ΔamyE::cat*_LOX. B0035_UtCAT was amplified via B617/B780 through UtCAT Gblock. *amyE* 3' arms with Cm^r were amplified by B776/B690.

*ΔamyE::cat*_LOX_R0 _UtCAT: *amyE* 5' arm with LOX was amplified via B685_V2/B778 through chromosomal DNA of PY79 ΔamyE::cat_LOX. R0_UtCAT was amplified via B779/B780 through UtCAT Gblock. *amyE* 3' arms with Cm^r were amplified by B776/B690.

*ΔamyE::cat*_UtCAT_L20 _LOX: *amyE* 5' arm with $P_{NBP3510}$ and *amyE* 3' arm with Cm^r were amplified by B685_V2/B784 and B776/B690 separately through chromosomal DNA of PY79 *ΔamyE::cat*_sfGFP. UtCAT was amplified through gblock via B785/B786. L20_LOX was amplified through *ΔamyE::cat*_CAT_L20_LOX via B787/B783.

B. subtilis transformation

Cementing PCR products were cleaned up by PB buffer before transformation. MC media was made at a 10x stock with final concentration of 14.036% K_2HPO_4 (w/v), 5.239% KH_2PO_4 (w/v),

20% glucose (w/v), 30mM trissodium citrate, 0.022% Ferric ammonium citrate (w/v), 2% potassium glutamate (w/v), 1% casein digest (Difco). The 10xMC stock was filtered and stored at -20 °C. To make1xMC media, supplemented 1xMC with 3mM $MgSO_4$. *B. subtilis* strains were restreaked one day before transformation. Single colonies were inoculated into 1ml 1xMC media followed by 37 °C, 220rpm shaking for 3-4h until turbid. Cementing pcr products were purified by 50ng PB buffer and directly added into 300ul of culture. Culture shaking was resumed at 37 °C for another 2.5h followed by centrifugation to get rid of 250μL supernatant. The remaining culture was plated on the LB plates with 5ug/ml Chloramphenicol. Multiple single colonies were picked the next day and restreaked on the selective LB plates to ensure integration. Colonies which grew successfully were picked and verified by Sanger sequencing.

SPP1 Phage Lysis and Transduction

The donor colony with was inoculated in 3ml TY broth (10g tryptone, 5g yeast extract, 5g NaCl per liter) and grew at 37 °C until the culture was turbid. SPPI phage dilutions were prepared from -2 to -6 in sterile tubes. 100ul of each dilution was added into a clean tube followed by the addition of 200ul turbid donor culture. Mixtures were incubated statically at 37 °C for 15mins. TY soft agar (5g agar/L) was melted during the incubation and supplemented with 10mM $MgSO_4$ and 0.1mM $MnSO_4$ as working concentration. 3ml soft agar was added into bacterial and phage mixture, and the mixture was vortexed. Tube contents were dumped onto the TY agar plate (15g agar/L) and the plate was swirled around to make sure the mixtures covered the entire plate surface. Plates were dried and incubated overnight at 37 °C. The next day lysates were harvested by adding 5ml TY media to appropriate plaques. Soft agar and TY broth were scraped and incubated at RT for 10min, then spun down at 4000rpm for 15mins. Lysate was filtered using 0.45um syringe filter into a new tube and 100ul chloroform was added for storage. For transduction experiments, lysates were prepared from the donor strains as described above. The recipient colony was inoculated in 3ml TY broth followed by shaking at 37 °C and 250 rpm until dense.1ml bacterial culture was mixed with 10ul phage stock followed by adding 9ml TY broth. The mixture was statically incubated at 37 °C in a water bath for 30mins. The mixture was then centrifuged at 4000rpm for 20min. The majority of Supernatant was discarded and the pellet was resuspended in the remaining volume. 100ul bacterial culture was plated on selective media with 10mM sodium citrate. Plates were then incubated overnight at 37 °C. The next day, 3-4 different colonies were restreaked onto selective plates without sodium citrate.

Catalase Activity Measurement

$1.6x10^9$ bacteria were pelleted and resuspended in 100ul 0.9% NaCl and 100ul 1% Triton X-100. The solution was transferred to FACS tubes. Subsequently, 100ul 3% hydrogen peroxide solution (Sigma, catalog #88597-100ML-F) was added to the solution followed by thorough mixing. After completion of each reaction, the height of oxygen forming foam was recorded by subtracting the height of solution.

Western Blotting

200ul bacterial pellet was collected by centrifugation and resuspended in 50ul 1xTE (10mM Tris-HCl, 1mM EDTA, pH8.0) with 1.5ul 50mg/ml lysozyme followed by 10mins incubation in 37 °C water bath. 10ul 6xSDS loading dye was added to suspension. The samples were first separated by 12% SDS-PAGE gel and then transferred to a nitrocellulose membrane (Fisher Scientific). The membranes were incubated with the Anti-FLAG epitope (DYKDDDDK, Biolegend, San Diego, CA, catalog# 637301) or Anti-HA epitope (ABclonal, Woburn, MA catalog# AE008) with 1:2000 dilution overnight in a cold room, and the secondary antibody anti-rat IgG HRP (Cell Signaling Technology, Danvers, MA, catalog# 7077) for Anti-FLAG or anti-mouse IgG HRP (Invitrogen, Waltham, MA, catalog# 626520) for Anti-HA with the same dilution at room temperature for 1 hr. Premixed Pierce™ 3,3'diaminobenzidine (DAB) substrate (Fisher Scientific) was used to detect the target proteins.

LOX Activity Measurement

Bacillus subtilis LOX, and sfGFP strains were inoculated in LB with 5ug/ml Cm at 30 °C overnight. Overnight cultures were diluted 10 times into 15ml fresh LB with 5ug/ml Cm followed by incubation at 37 °C until OD_{600}=0.8. Pellets were collected by centrifugation at 4000rpm 20°C for 10 mins and washed with PBS three times. 100ul 0.5 M perchloric acid (PCA) was pre-aliquoted in a 96-well V bottom plate and placed on ice. The pellet was resuspended with PBS and the OD_{600} was adjusted to 1. Bacterial culture and lactate standards at concentrations of 5mM, 2.5mM, 1.25mM, 0.625mM, 0mM were added to the corresponding positions of the layout in a 2ml deep well plate. Na-L-lactate (Fisher, catalog# AAL1450006) was added to the corresponding bacterial suspension with 5mM working concentration. 100ul reaction mixture was mixed and transferred to pre-aliquoted PCA on ice as the baseline. The 96-well deep well plate was kept in a shaker at 37 °C 220rpm to collect samples at desired timepoints. The V-bottom plates were spun down at 4 °C 4000rpm for 10mins after 30mins incubation on ice. 150ul supernatant was transferred into a new 96-well cell plate and neutralized by 30ul 2.3M $KHCO_3$ followed by overnight precipitation. The plates were centrifuged at 4000rpm 4C the next day for 10mins to collect the samples for

pyruvate or lactate detection. For lactate detection, 10ul of each sample and water blanks were added to 96-flat black well plates with three technical repeats. 185ul Lactate detection buffer (100mM Hydrazine dihydrochloride, 100mM glycine, 0.5mM NAD+, pH 10) was added to each well followed by 15mins incubation. The plate was read at excitation 340, emission 460 as the baseline. 5ul 8U/ml L-Lactic Dehydrogenase (LDH) from rabbit muscle Type II, ammonium sulfate suspension (Sigma L2500) was added to all the wells followed by 250rpm shaking for 5mins to mix well, and plates were kept in the dark. Plates were then incubated in the dark for 2h and read.

Spore Preparation

Bacterial culture was plated on selective 2*Schaeffer's medium-glucose plates followed by 1-week 37 °C incubation[50]. Spores were scraped from the plate to centrifuge tubes and were then washed by resuspension in ddH_2O. Spores were then pelleted via centrifugation at 5000rpm for 10min at RT. The pellet was then resuspended in ddH2O followed by three cycles of 1 min sonication at 20 W and 2,100 Joules, and 1 min rest. Spores were subjected to 1min sonication followed by1min rest. This cycle was repeated step three times a day for 3days. Spores were aliquoted at 10^9 CFU/ml each tube and storage in -80C for later use.

In Vivo Lactate Challenge

All animal experiments were conducted under the guideline of the IACUC, Northeastern University, Boston, MA. Five female C57BL/6 mice (Jackson Laboratories) or CD-1 mice (Charles River Laboratories) were housed in a single cage for each condition. 6 to 8-week-old mice were gavaged with either PBS or 200ul bacterial and spore mixture (10^{10} vegetative cells plus 10^8 spores) of the corresponding bacterial strain for 3 days in row. 20mins after the 3rd oral gavage, baseline blood lactate level was measured by Lactate Plus: Blood Lactate Measuring Meter-Version 2 (NovaBiomedical) and Lactate Plus Meter Test Strips (NovaBiomedical, catalog# 40813) through tail nick under anesthesia. Na-L-lactate was administered subcutaneously via injection in the back area at a dose of 2.3g/kg body weight. Blood lactate was measured at desired timepoints under anesthesia.

CFU Counting for Fecal Samples

Stools were collected before 1st gavage, and 1day, 3 days, 5days, 7 days, 15 days, 18 days after 1st gavage. Fecal samples were placed in 300ul sterile PBS buffer followed by 15mins incubation. The mixture was homogenized by micro tissue homogenizer. The solution was obtained by centrifugation and applied to LB agar with 7.5ug/ml chloramphenicol, 0.25ug/ml gentamycin, and

0.25ug/ml erythromycin. Plates were incubated at 37 °C for 12-16 h. CFU was determined by standard CFU counting method.

Genomic DNA Extraction from Feces

C57BL/6 mouse feces were collected before 1st gavage, and 1day, 3 days, 5days, 7 days, after 1st gavage. Feces were immediately frozen in liquid nitrogen and saved in -80 °C for later use. Genomic DNA was extracted by Quick-DNA Fecal/Soil Microbe Miniprep Kit (Zymo, catalog# D6010) following the instructions.

16S rRNA Gene Sequencing and Analysis

16s rRNA analyses were performed both in-house and by Novogene, China. gDNA concentration was measured with 1% agarose gels. According to the concentration, DNA was diluted to 1ng/μL using sterile water. 16S rRNA V4 specific primers are 515F (5'-GTGCCAGCMGCCGCGGTAA-3') and 806A (5'-GGACTACHVGGGTWTCTAAT-3'). All PCR reactions were carried out in 30μL reactions with 15μL of Phusion® High-Fidelity PCR Master Mix (New England Biolabs), 0.2μM of forward and reverse primers, and about 10 ng template DNA. Thermal cycling is started with the initial denaturation at 98 for 1 min, followed by 30 cycles of denaturation at 98°C for 10 s, annealing at 50°C for 30 s, and elongation at 72°C for 60 s. Finally within 72°C for 5 min. PCR products were mixed with equal volume of SYB Green loading buffer and operated electrophoresis on 2% agarose gel for quantification and qualification followed by purification with GeneJET Gel Extraction Kit (Thermo Scientific). Sequencing libraries were generated using NEB Next® Ultra™ DNA Library Prep Kit for Illumina (NEB, USA) following manufacturer's recommendations and index codes were added. The library quality was assessed on the Qubit@ 2.0 Fluorometer (Thermo Scientific) and Agilent Bioanalyzer 2100 system. At last, the library was sequenced on an Illumina HiSeq 2500 platform, generating 250 bp paired-end reads. For taxa relative abundance outcomes, qualified reads were filtered by QIIME software to obtain clean tags. All tags were compared with the reference database using UCHIME algorithm to obtain effective tags only which were used for diversity analysis. For diversity analyses, FASTA files were processed with DADA2 for R, with primer sorted and demultiplexed sequences filtered and trimmed at truncation lengths of 240 and 160 bp for forward and reverse reads respectively with a minimum quality score of 20. Following merging and removing of chimeric reads, taxonomy was assigned as Amplicon Sequence Variants (ASVs) with Silva v138 taxonomic database. Using

phyloseq for R, ASVs not present at least 5 times in 50% of samples were pruned, and in all outcomes aside from alpha diversity, reads were rarefied to even sampling depth.

Mouse Proinflammatory Focused Luminex Assay

All plasma samples were collected from C57BL/6 mice. Baseline (0h) plasma was isolated before the 1st oral administration followed by plasma collection at 24h, 72h, and 7 days post-1st oral gavage. Plasma was collected by centrifugation at 3000g for 30mins, 4 °C. The plasma was transferred to clean 0.65ml tubes for Luminex Assay (MDF10) through Eve Technology (Canada).

Liver Enzymes Measurements

All serum samples were collected from C57BL/6 mice. Baseline (0h) serum was isolated before the 1st oral administration followed by serum collection at 24h, 72h, and 7 days after 1st oral gavage. Serum were storage in -80 °C until use. AST and ALT levels were sent to University of Michigan IVAC facility for mini liver chemistry panel (MI1015) analysis.

Statistical Analysis

All statistical analyses were performed using GraphPad Prism 9 (San Diego, CA, USA). Data were analyzed with one-way or two-way analysis of variance (ANOVA) for statistical significance.

Acknowledgement

This work was supported by National Institute of Biomedical Imaging and Bioengineering (R21EB030769) and CDMRP PRMRP (W81XWH-21-1-0016). WBSGFP were kindly provided by Prof. Xin Yan from Nanjing Agricultural University, China. SPP1 phage was a generous gift by Professor Dan Kearns from Indiana University Bloomington. We would like to express our gratitude to Professor Sara Rouhanifard at Northeastern University's Department of Bioengineering for generously sharing her lab's plate reader with us; Professor Ke Zhang at Northeastern University's Department of Chemistry for sharing his lab's equipment and space. We also wish to thank my colleague Morgen Benson for her contribution to the sfGFP construct during the lab rotation.

Conflict of Interest

A provisional patent has been filed by Northeastern “INV-23011, “Engineer probiotics to sense and respond to lactic acid buildup in diverse diseases”.

Author contribution

JL conceived the ideas and supervised the experiments. MY designed and conducted all the experiments. NH assisted with 16S rRNA α- and β-diversity analysis and provided the figures. JY assisted with material preparation and plate reading for LOX activity *in vitro* tests, as well as phage transduction. MG assisted with spore preparation and western blotting. ZW prepared the *B. subtilis* vegetative cells and assisted in measuring lactate changes. PC provided guidance for mice restraint and blood collection. SY provided guidance for mice oral administration. JC developed the lactate *in vitro* assay. All authors contributed to the discussion of the results and the writing and editing of the manuscript.

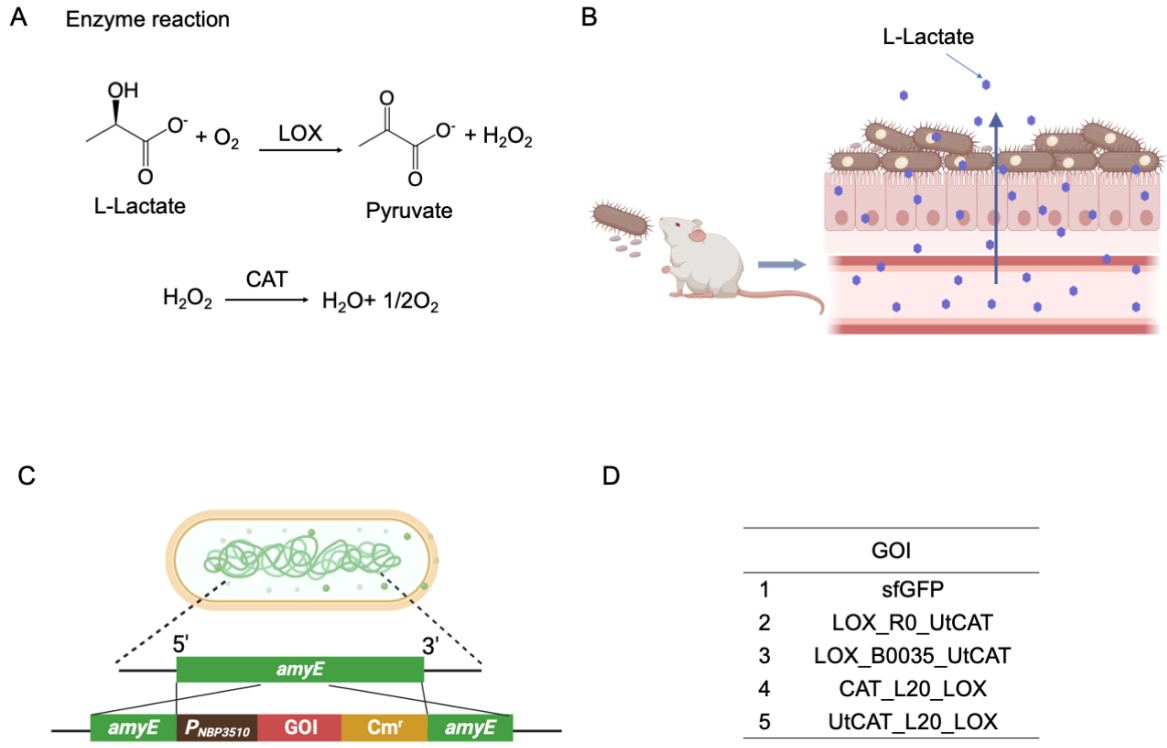

	GOI
1	sfGFP
2	LOX_R0_UtCAT
3	LOX_B0035_UtCAT
4	CAT_L20_LOX
5	UtCAT_L20_LOX

Figure 1. Schematic diagram and genomic integration of lactate oxidase and catalase in multiple *B. subtilis* strains (A) Enzyme reactions of lactate oxidase (LOX) and catalase (CAT). (B) Engineered *B. subtilis* strains were programmed to express Lactate Oxidase (LOX), facilitating the conversion of lactate to pyruvate. (C) The genetic design involved the incorporation of constitutively expressed transgenes in a nonessential gene, *amyE* locus of the *B. subtilis* chromosome. The target gene of interest was driven by the $P_{NBP3510}$ promoter, and it was followed by a chloramphenicol-resistant gene. (D) The construction list used in this study included the following enzymes: LOX (lactate oxidase from), CAT (catalase from *E. coli*), and UtCAT (catalase from *Ureibacillus thermosphaericus*). R0 and B0035 are synthetic ribosome binding sequence (RBS). L20, a 20-amino acid peptide linker between two proteins. This figure was created by BioRender.

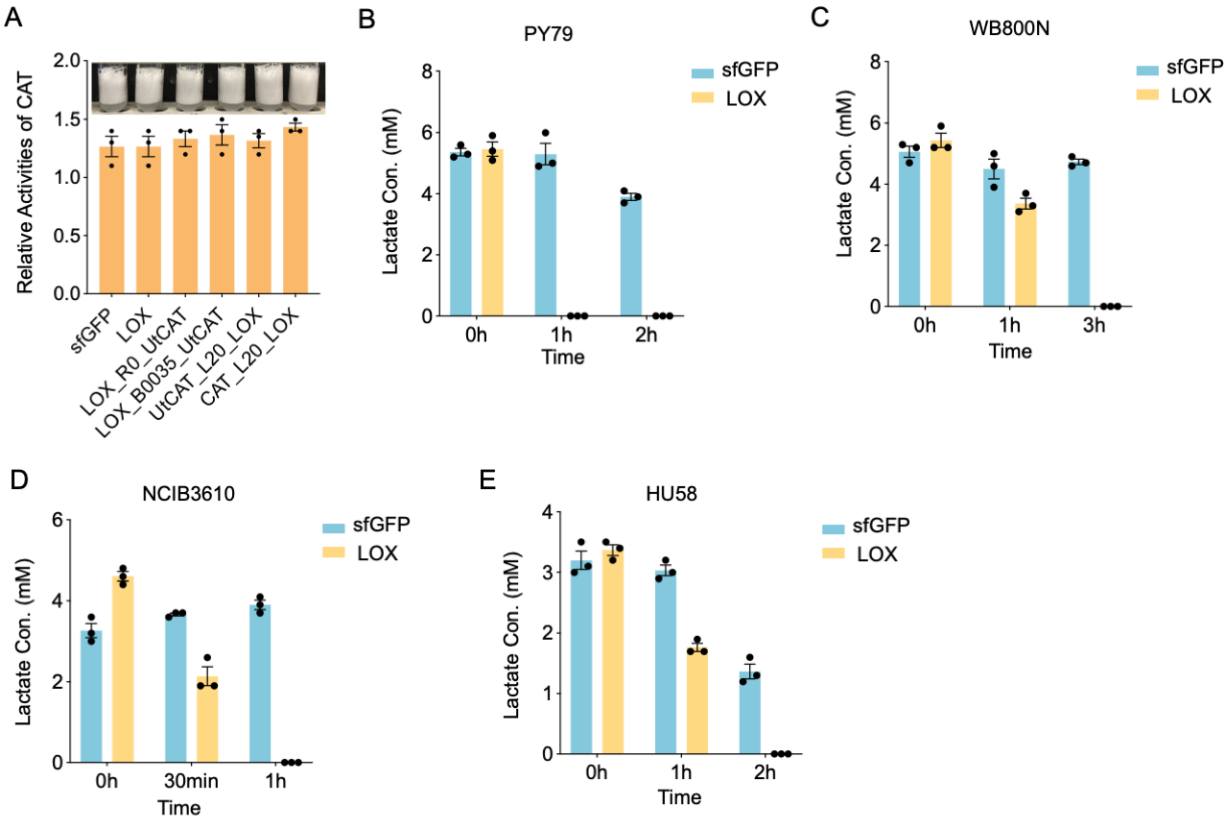

Figure 2. *B. subtilis* expressing LOX remove extracellular lactate.

(A) *B. subtilis* PY79 exhibited extracellular catalase activities regardless of the presence of an additional copy of transgene (UtCAT or CAT). The inset figure depicts the foam height resulting from the catalytic reaction between catalase and H_2O_2. Specifically, 1.6 x 10^9 *B. subtilis* cells were suspended in 100 µL of 0.9% saline and 100 µL of 1% Triton X-100 before being transferred to 5 ml culture tubes. Subsequently, 100 µL of 3% hydrogen peroxide was introduced to the mixture and thoroughly mixed. Following the cessation of foam formation, the height of the O_2-evolving foam within the test tube was measured using a ruler. *B. subtilis*^{LOX} completely consumed exogenous lactate within 1 hour for PY79 (B) and NCIB3610 (D). 2 hours, and 3 hours respectively for WB800N (C), and HU58 (E). n=3, N=3.

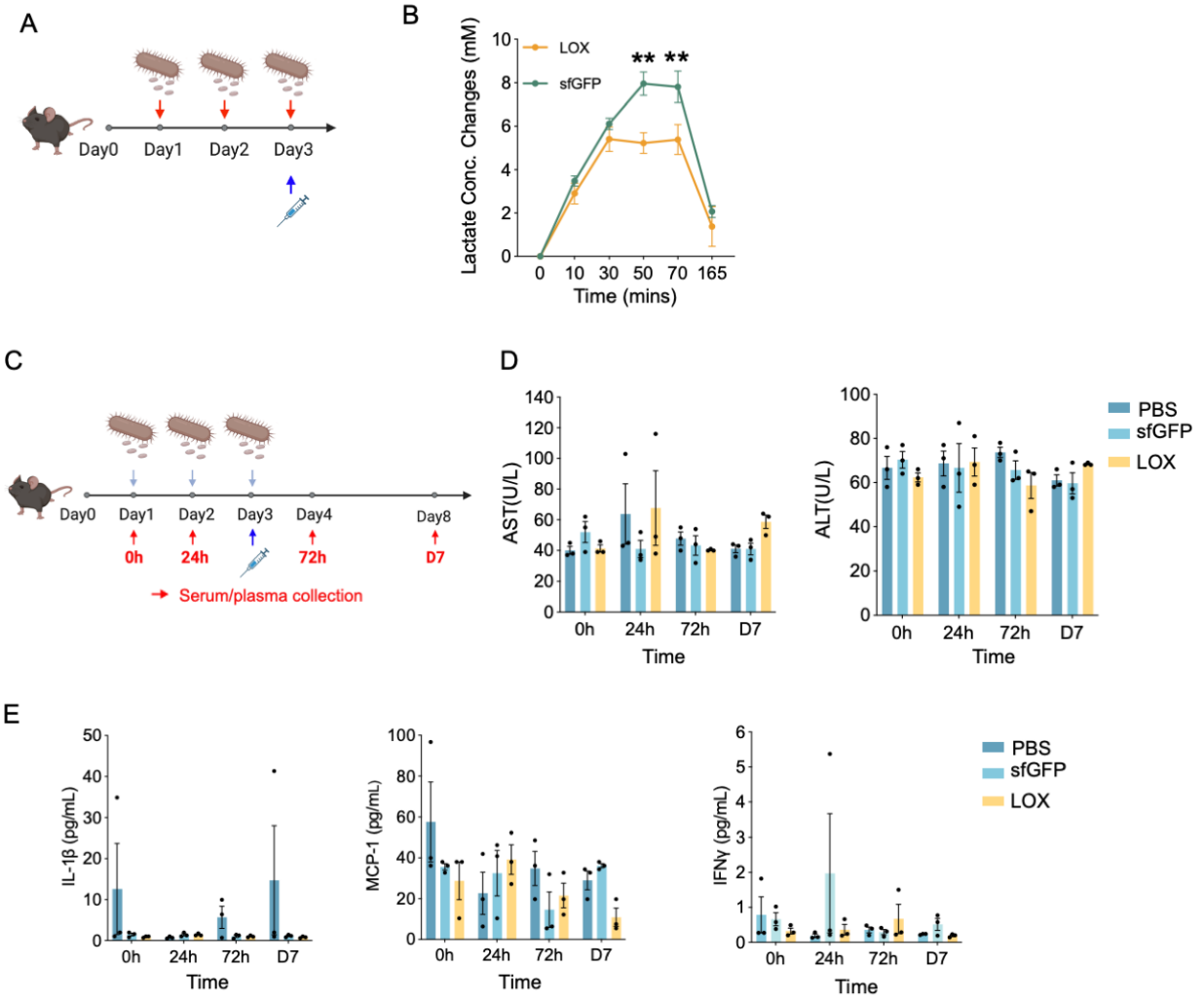

Figure 3. Oral administration of *B. subtilis*^{LOX} significantly reduced the blood lactate elevation. (A) Schematic diagram of the lactate challenge procedure. For three days, female C57BL/6 mice were orally administered 200 uL of a mixture of spores and vegetative cells. Twenty minutes after the last gavage and a baseline blood lactate measurement, 2.3g/kg body weight Na-L-lactate was injected subcutaneously. (B) Time course measurements of blood lactate concentration in response to injection. Lactate concentration changes=current lactate concentration-baseline concentration. Data was analyzed by the Two-Way ANOVA followed by Bonferroni's multiple comparisons test, **p<0.01. Date are means ± SEM. n=10 mice for each treatment. (C) Schematic of timepoints for serum and plasma collection. 0h was collected before the first oral gavage. 24h, 72h and D7 were collected at desired the timepoint after the first oral gavage. (D) Liver function represented by circulating ALT and AST levels. ALT and AST concentrations in plasma of healthy mice range from 24.3 - 115.25 U/L and 39.55 - 386.05 U/L respectively. n=3 mice for each treatment. Data are means ± SEM. (E) Concentrations of proinflammatory cytokines and chemokines in mouse plasma were not affected by treatment or

timepoint when measured by Luminex Assay. IL, interleukin; MCP, monocyte chemoattractant protein; IFN, interferon. n=3 for each treatment. Data are means ± SEM.

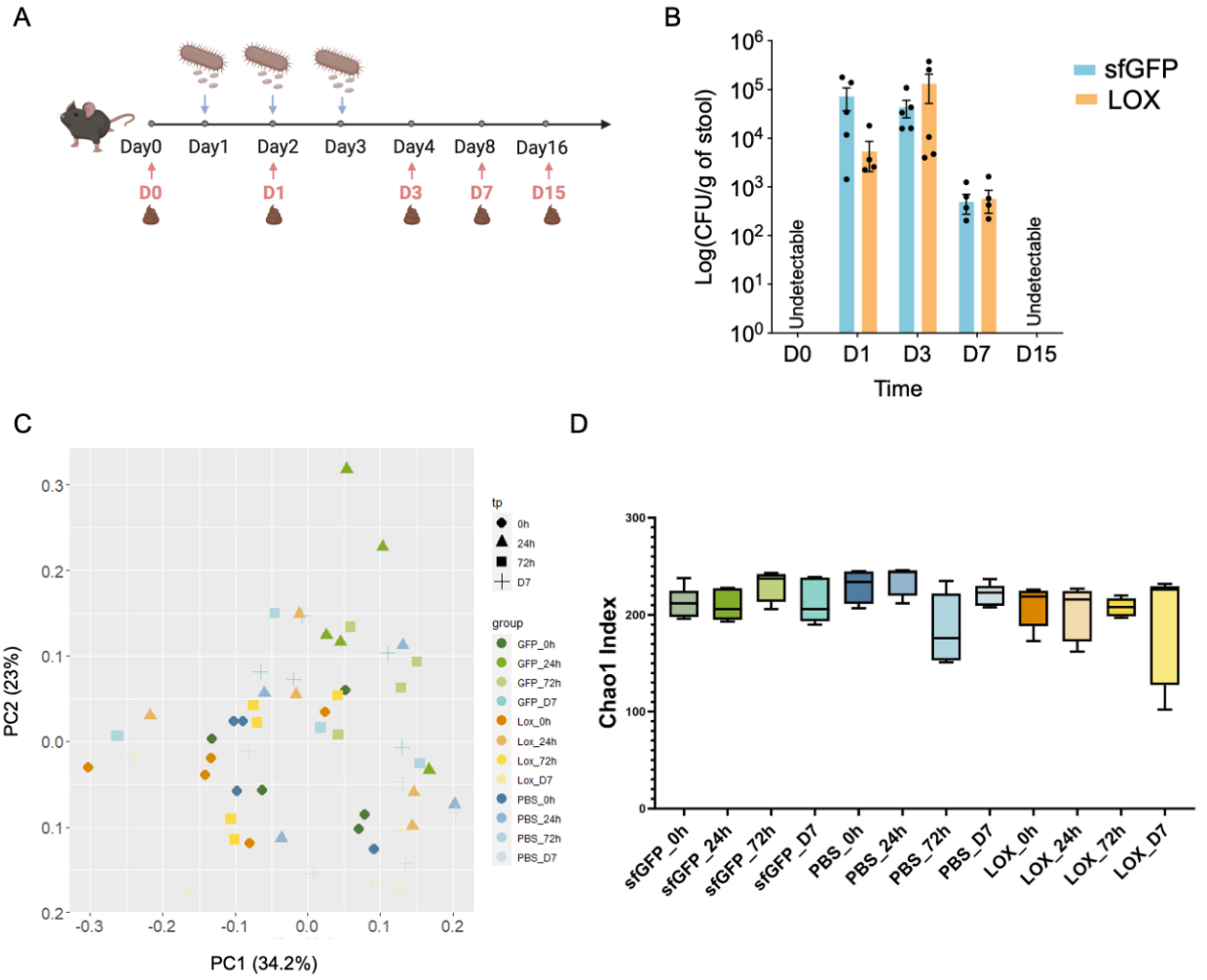

Figure 4. Supplement of engineered *B. subtilis* didn't disturb intestinal microbiome community. (A) Schematic of the experimental procedure. (B) The relative abundance of *B. subtilis* increased upon daily oral gavage of a mixture of 10^{10} vegetative cells and 10^{8} spores at Day 1, 2, and 3. However, *B. subtills* decreased by D7 and was undetectable by D15. There are no significant differences between each group. N=5 per treatment per timepoint. (C) Weighted Unifrac Principal Coordinate Analysis (PCoA) found no differences in community composition between timepoints or treatment group. n=5 for each treatment, P>0.05. (D) Chao1 index of Alpha diversity was unaffected by treatment or timepoint. n=5 for each treatment. P=0.16 and 0.67 for treatment and timepoint respectively.

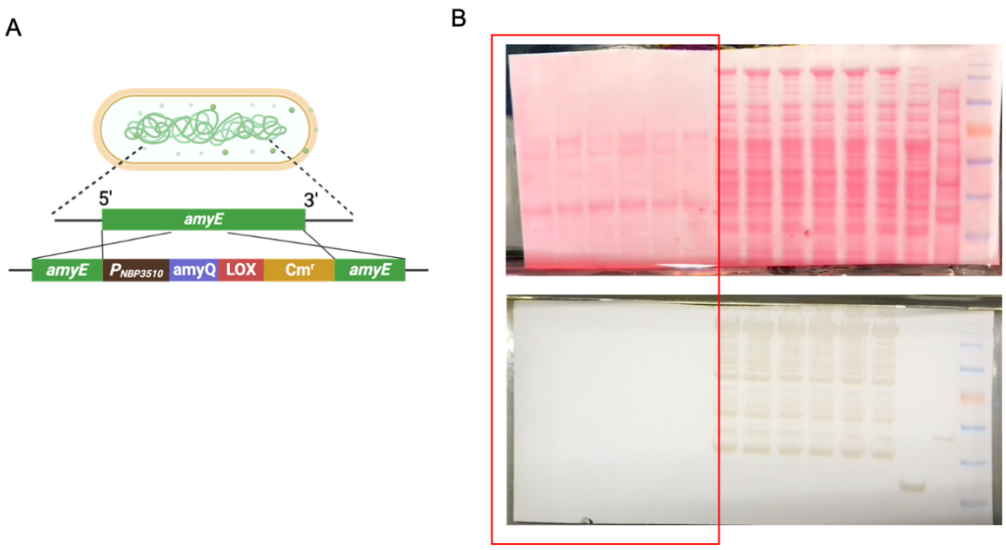

Supplementary Figure 1: *B. subtilis* failed to secret LOX extracellularly. (A) The genetic design for extracellular LOX secretion differs from intracellular expression. Specifically, an *amyQ* secretion signal sequence was incorporated before the LOX sequence. (B) LOX was not detected in the supernatant through Western Blot (red rectangle).

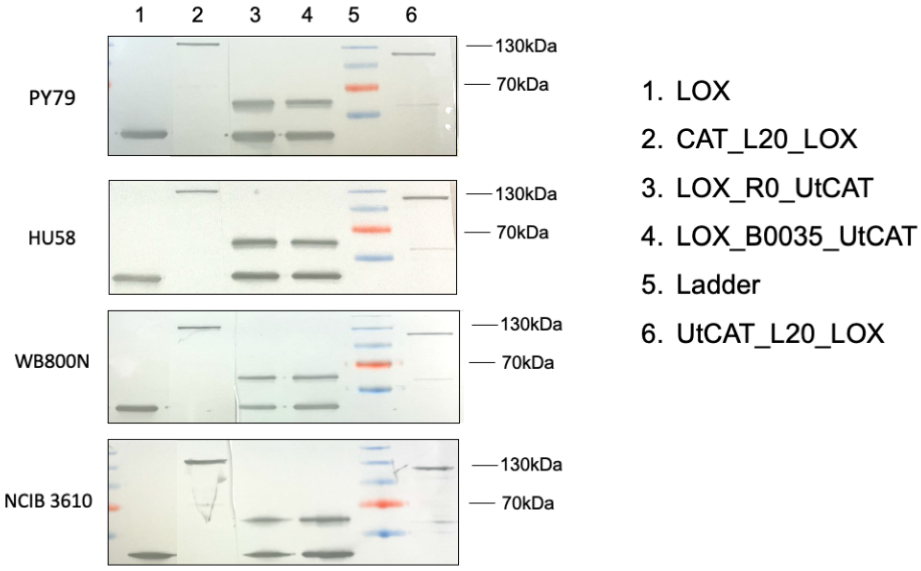

Supplementary Figure 2: Western Blot of expressed enzymes in various *B. subtilis* strains. The predicted molecular weight for LOX, UtCAT, CAT_L20_LOX, UtCAT_L20_LOX are 41kDa, 59kDa, 120kDa, and 101kDa. The data are representative of at least 3 biological repeats with similar results. The membranes were cut and merged.

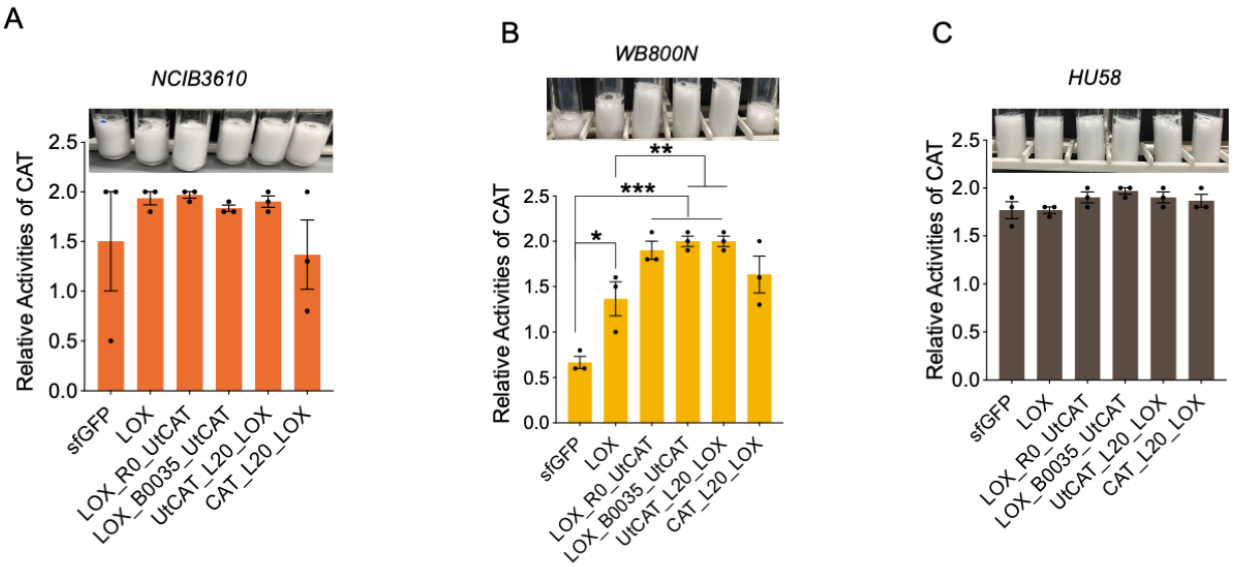

Supplementary Figure 3: The catalase activities of different *B. subtilis* strains (A) NCIB3610, (B) WB800N and (C) HU58. Images indicate foam formation due to trapped oxygen gas by surfactant, resulting from the breakdown of hydrogen peroxide catalyzed by endogenous catalase (sfGFP or LOX only) or overexpression of *E. coli* catalase (CAT) or *U. thermosphaericus* catalase (UtCAT). *B. subtilis* were resuspended in 100ul 0.9% NaCl and 100 ul 1% Triton X-100 and transferred to FACS tubes. 100 ul of 3% hydrogen peroxide was added to the mixture and mixed thoroughly. The height of O_2- forming foam in the test tube was measured by a ruler. N=3. Data was analyzed by unpaired t-test, $*p < 0.05$, $**p < 0.01$, $***p < 0.001$. Date are means ± SEM.

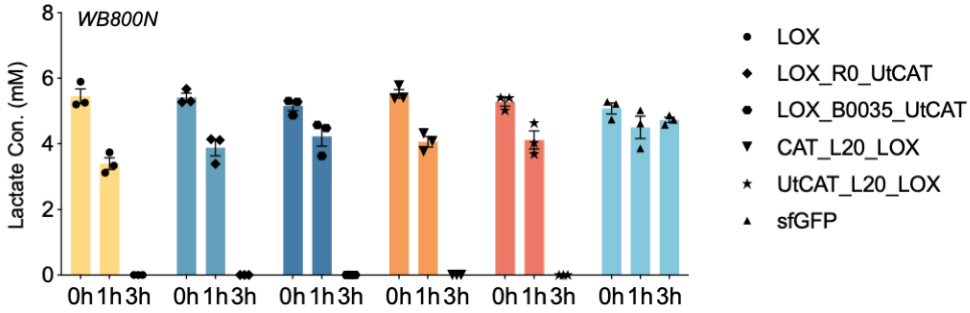

Supplementary Figure 4: WB800N *B. subtilis*^{LOX} constructs could completely consumed exogenous lactate within 1 hour and exhibited similar conversion capabilities. N=3. Date are means ± SEM.

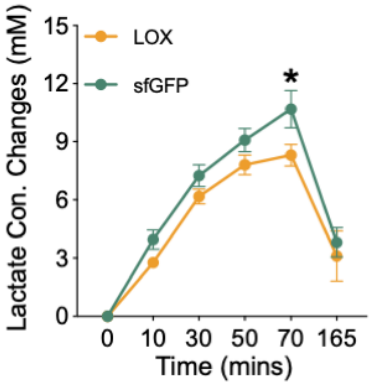

Supplementary Figure 5: Engineered *B. subtilis* PY79 could significantly reduce the blood lactate elevation in CD-1 mice. A mixture of 10^{10} engineered PY79 vegetative cells and 10^{8} spores were administered to female CD-1 mice for 3 days. 20 minutes after the third dose, baseline blood lactate level (0min) was measured followed by subcutaneous injection with 2.3g per kg body weight Na-L-lactate. Blood lactate concentrations were quantified by a portable lactate meter at different timepoints. Lactate concentration changes = lactate concentration minus the baseline lactate concentration per mouse. Data were analyzed by the two-way ANOVA followed by Bonferroni's multiple comparisons test , *p<0.05. Date = means ± SEM. n=10 mice for each treatment group.

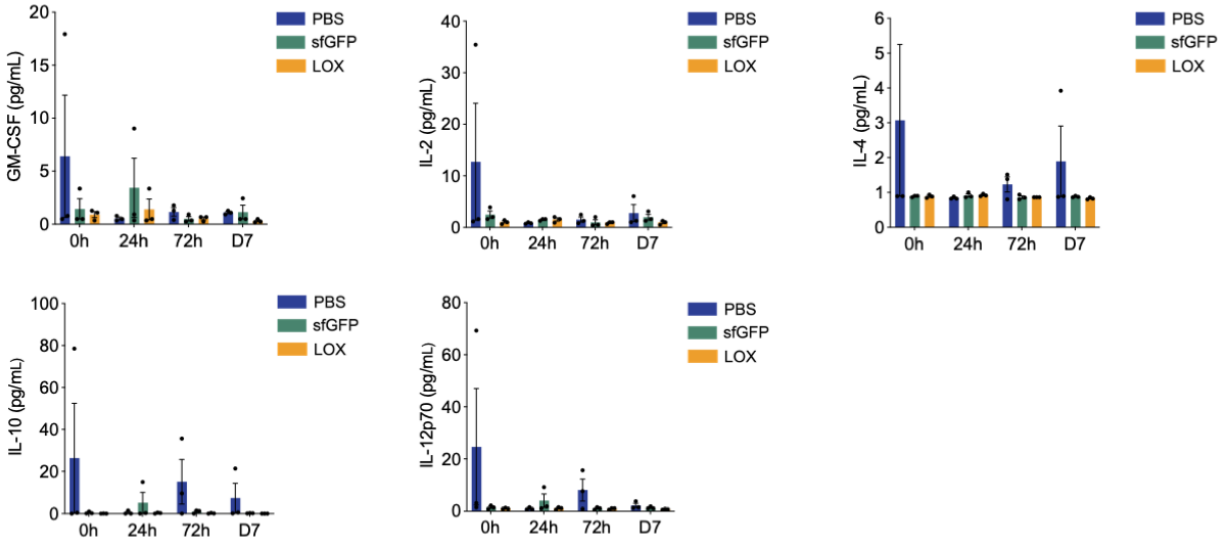

Supplementary Figure 6: Profiling of proinflammatory cytokines (GM-CSF, IL-2, IL-4, IL-10 and IL-12p70) in the plasma of treated mice indicate lack of side effects. Cytokines were quantified by the Luminex assay.

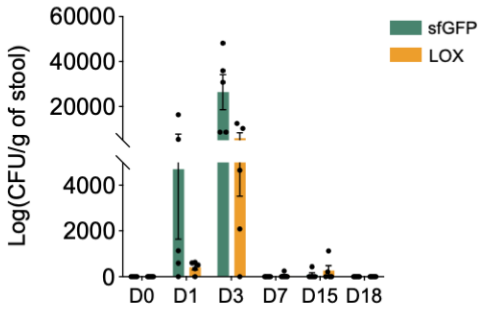

Supplementary Figure 7: The abundance of engineered *B. subtilis* PY79 after first oral gavage in CD-1 mice. No CFU were recovered at 18 days post the first oral gavage. There are no significant differences between each group. n=5 per treatment per timepoint. Date are means ± SEM.

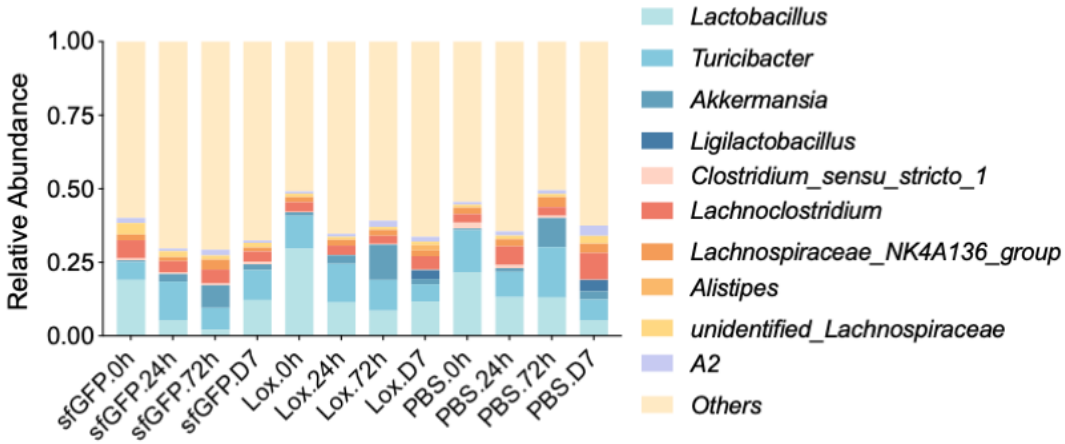

Supplementary Figure 8: Relative abundance of the top 10 genera in each treatment group across timepoints did not include *B. subtilis*. n=5 for each treatment.

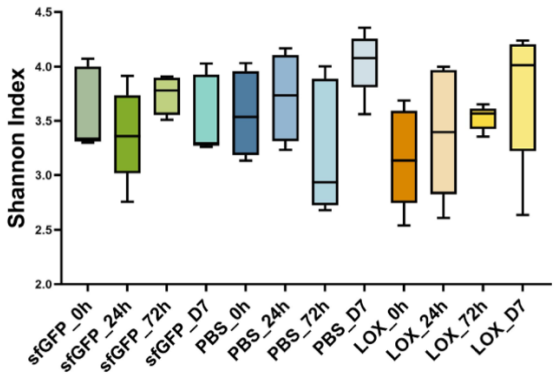

Supplementary Figure 9: Shannon index of α-diversity analysis suggests there were no differences in community evenness between *B. subtilis* and PBS groups in C57BL/6 mice. P=0.488 and 0.137 for treatment and time point respectively. n=5 for each treatment.

Supplemental Table 1: primers used in this study

Primer	Sequences 5' to 3'	Description	Construct
B685_V2	TGCTTACGATGTACGACAGGGGG	amyE_up_fwd	*ΔamyE ::cat*_sfGFP
B742	CTAAAAATTTGTAATTAAGAAGGAGTGATTACcgatcagaccagtttttaatttg	amyE_up_rev	
B741	GTAATCACTCCTTCTTAATTACAAATTTTTAG	$P_{NBP3510}$_sfGFP_fwd	
B747	GCGTAAGGAAATCCATTATGTACTATTTttcatatatttggctgcggtag	$P_{NBP3510}$_sfGFP_rev	
B746	AAATAGTACATAATGGATTTCCTTACGC	*cat*_amyE_down_fwd	
B690	CATCCTTGCAGGGTATGTTTCTCTTTG	amyE_cat__down_rev	
B774	tcaatgtcattgttattcatACGTTCTACCTTTGTCAAAC	amyE_$P_{NBP3510}$_rev	*ΔamyE ::cat*_LOX
B775	AACGTatgaataacaatgacattga	LOX_fwd	
B777	GGACGTCGACTCTAGAttactatttgtcatcgtcg	LOX_rev	
B776	tagtaaTCTAGAGTCGACGTCC	*cat*_amyE_down_fwd	
B781	tcgtcgtctttgtagtccatACGTTCTACCTTTGTCAAAC	amyE_$P_{NBP3510}$_rev	*ΔamyE ::cat*_CAT_L20_LOX
B782	GTatggactacaaagacgacgat	CAT_fwd	
B218	caccttccgagccaccgccctcggagcctcccgcaccacttgcggcaggaattttgtcaatc	CAT_rev	
B219	ggtggctcggaaggtgggacgagcggcgccaccaataacaatgacattgaatataatgc	L20_LOX_fwd	
B783	GGACGTCGACTCTAGAttactagtattcataaccgtatg	L20_LOX_rev	
B614	agtattctcctctttaatctctagattactatttgtcatcgtcg	LOX _rev	*ΔamyE ::cat*_LOX_B0035_UtCAT
B617	agagattaaagaggagaatactagatgaccaatattaatgataaacg	B0035_UtCAT _fwd	
B780	GGACGTCGACTCTAGAttactatgcatagtctggc	B0035_UtCAT _rev	

B778	gtttgtcctccttattagttaatcttactatttg tcatcgtcg	LOX_Rev	*ΔamyE ::cat*_LOX_R 0 _UtCAT
B779	gattaactaataaggaggacaaacatg accaatattaatgataaacg	R0_UtCAT_Fwd	
B780	GGACGTCGACTCTAGAttacta tgcatagtctggc	R0_UtCAT_rev	
B784	TTATCATTAATATTGGTCATA CGTTCTACCTTTGTCAAAC	amyE_$P_{NBP3510}$_rev	*ΔamyE ::cat*_UtCAT_ L20 _LOX
B785	TAGAACGTATGACCAATATTA ATGATAA	UtCAT _fwd	
B786	ctcccgcaccacttgcTGCATAGTC TGGCACGTC	UtCAT _rev	
B787	TATGCAgcaagtggtgcgggag	L20_LOX_fwd	

Reference

1. Adeva-Andany, M., et al., *Comprehensive review on lactate metabolism in human health.* Mitochondrion, 2014. **17**: p. 76-100.
2. Zúñiga, A., et al., *Engineered l-Lactate Responding Promoter System Operating in Glucose-Rich and Anoxic Environments.* ACS Synthetic Biology, 2021. **10**(12): p. 3527-3536.
3. Villar, J., J.H. Short, and G. Lighthall, *Lactate Predicts Both Short- and Long-Term Mortality in Patients With and Without Sepsis.* Infectious Diseases: Research and Treatment, 2019. **12**: p. 1178633719862776.
4. Manosalva, C., et al., *Role of Lactate in Inflammatory Processes: Friend or Foe.* Frontiers in Immunology, 2022. **12**.
5. Haller, H.L., et al., *Oxygen, pH, Lactate, and Metabolism—How Old Knowledge and New Insights Might Be Combined for New Wound Treatment.* Medicina, 2021. **57**(11): p. 1190.
6. Cai, M., et al., *Understanding the Contribution of Lactate Metabolism in Cancer Progress: A Perspective from Isomers.* Cancers, 2023. **15**(1): p. 87.
7. Steinman, M.Q., V. Gao, and C.M. Alberini, *The Role of Lactate-Mediated Metabolic Coupling between Astrocytes and Neurons in Long-Term Memory Formation.* Frontiers in Integrative Neuroscience, 2016. **10**.
8. Nørlinger, T.S., et al., *Hyperbaric oxygen therapy reduces renal lactate production.* Physiological Reports, 2017. **5**(6): p. e13217.
9. Rajan, S., et al., *Effect of lactate versus acetate-based intravenous fluids on acid-base balance in patients undergoing free flap reconstructive surgeries.* Journal of Anaesthesiology Clinical Pharmacology, 2017. **33**(4): p. 514-519.
10. Sada, N., et al., *Targeting LDH enzymes with a stiripentol analog to treat epilepsy.* Science, 2015. **347**(6228): p. 1362-1367.
11. Pucino, V., D. Cucchi, and C. Mauro, *Lactate transporters as therapeutic targets in cancer and inflammatory diseases.* Expert Opinion on Therapeutic Targets, 2018. **22**(9): p. 735-743.
12. Patgiri, A., et al., *An engineered enzyme that targets circulating lactate to alleviate intracellular NADH:NAD+ imbalance.* Nature Biotechnology, 2020. **38**(3): p. 309-313.
13. Ho, C.L., et al., *Engineered commensal microbes for diet-mediated colorectal-cancer chemoprevention.* Nature Biomedical Engineering, 2018. **2**(1): p. 27-37.
14. Fujii, T., et al., *Efficacy of pyruvate therapy in patients with mitochondrial disease: A semi-quantitative clinical evaluation study.* Molecular Genetics and Metabolism, 2014. **112**(2): p. 133-138.
15. Inoue, T., et al., *Pyruvate Improved Insulin Secretion Status in a Mitochondrial Diabetes Mellitus Patient.* The Journal of Clinical Endocrinology & Metabolism, 2016. **101**(5): p. 1924-1926.
16. Scheiman, J., et al., *Meta-omics analysis of elite athletes identifies a performance-enhancing microbe that functions via lactate metabolism.* Nature Medicine, 2019. **25**(7): p. 1104-1109.
17. Brutscher, L.M., et al., *Preclinical Safety Assessment of Bacillus subtilis BS50 for Probiotic and Food Applications.* Microorganisms, 2022. **10**(5): p. 1038.

18. Cho, W.-I. and M.-S. Chung, *Bacillus spores: a review of their properties and inactivation processing technologies.* Food Science and Biotechnology, 2020. **29**(11): p. 1447-1461.
19. Zhang, X., et al., *Applications of Bacillus subtilis Spores in Biotechnology and Advanced Materials.* Applied and Environmental Microbiology, 2020. **86**(17): p. e01096-20.
20. Yang, M., et al., *Engineering Bacillus subtilis as a Versatile and Stable Platform for Production of Nanobodies.* Appl Environ Microbiol, 2020. **86**(8).
21. Su, Y., et al., *Bacillus subtilis: a universal cell factory for industry, agriculture, biomaterials and medicine.* Microbial Cell Factories, 2020. **19**(1): p. 173.
22. Borriss, R., et al., *Bacillus subtilis, the model Gram-positive bacterium: 20 years of annotation refinement.* Microbial Biotechnology, 2018. **11**(1): p. 3-17.
23. Bernardeau, M., et al., *Importance of the gastrointestinal life cycle of Bacillus for probiotic functionality.* Journal of Food Science and Technology, 2017. **54**(8): p. 2570-2584.
24. Lu, J., et al., *Co-expression of alcohol dehydrogenase and aldehyde dehydrogenase in Bacillus subtilis for alcohol detoxification.* Food and Chemical Toxicology, 2020. **135**: p. 110890.
25. Souza, C.C.d., et al., *The multifunctionality of expression systems in Bacillus subtilis: Emerging devices for the production of recombinant proteins.* Experimental Biology and Medicine, 2021. **246**(23): p. 2443-2453.
26. Hartl, B., et al., *Development of a new integration site within the Bacillus subtilis chromosome and construction of compatible expression cassettes.* J Bacteriol, 2001. **183**(8): p. 2696-9.
27. Piewngam, P., et al., *Probiotic for pathogen-specific Staphylococcus aureus decolonisation in Thailand: a phase 2, double-blind, randomised, placebo-controlled trial.* The Lancet Microbe, 2023. **4**(2): p. e75-e83.
28. Piewngam, P., et al., *Pathogen elimination by probiotic Bacillus via signalling interference.* Nature, 2018. **562**(7728): p. 532-537.
29. Hou, Q., et al., *Bacillus subtilis programs the differentiation of intestinal secretory lineages to inhibit Salmonella infection.* Cell Reports, 2022. **40**(13): p. 111416.
30. Appala Naidu, B., et al., *Lyophilized B. subtilis ZB183 Spores: 90-Day Repeat Dose Oral (Gavage) Toxicity Study in Wistar Rats.* Journal of Toxicology, 2019. **2019**: p. 3042108.
31. Marzorati, M., et al., *Bacillus subtilis HU58 and Bacillus coagulans SC208 Probiotics Reduced the Effects of Antibiotic-Induced Gut Microbiome Dysbiosis in an M-SHIME® Model.* Microorganisms, 2020. **8**(7): p. 1028.
32. Duc, L.H., et al., *Characterization of Bacillus Probiotics Available for Human Use.* Applied and Environmental Microbiology, 2004. **70**(4): p. 2161-2171.
33. Wickramasuriya, S.S., et al., *Orally delivered Bacillus subtilis expressing chicken NK-2 peptide stabilizes gut microbiota and enhances intestinal health and local immunity in coccidiosis-infected broiler chickens.* Poultry Science, 2023. **102**(5): p. 102590.
34. Hu, Y., et al., *Bacillus subtilis Strain Engineered for Treatment of Soil-Transmitted Helminth Diseases.* Applied and Environmental Microbiology, 2013. **79**(18): p. 5527-5532.

35. Tam, N.K.M., et al., *The Intestinal Life Cycle of Bacillus subtilis and Close Relatives.* Journal of Bacteriology, 2006. **188**(7): p. 2692-2700.
36. Cartman, S.T., R.M.L. Ragione, and M.J. Woodward, *Bacillus subtilis Spores Germinate in the Chicken Gastrointestinal Tract.* Applied and Environmental Microbiology, 2008. **74**(16): p. 5254-5258.
37. Zhou, C., et al., *Promoter engineering enables overproduction of foreign proteins from a single copy expression cassette in Bacillus subtilis.* Microb Cell Fact, 2019. **18**(1): p. 111.
38. Li, G., et al., *Enzymatic preparation of pyruvate by a whole-cell biocatalyst coexpressing l-lactate oxidase and catalase.* Process Biochemistry, 2020. **96**: p. 113-121.
39. Iwase, T., et al., *A Simple Assay for Measuring Catalase Activity: A Visual Approach.* Scientific Reports, 2013. **3**(1): p. 3081.
40. Naclerio, G., et al., *Bacillus subtilis Vegetative Catalase Is an Extracellular Enzyme.* Applied and Environmental Microbiology, 1995. **61**(12): p. 4471-4473.
41. Moore, T., et al., *Oral administration of Bacillus subtilis strain BSB3 can prevent heat stress-related adverse effects in rats.* Journal of Applied Microbiology, 2014. **117**(5): p. 1463-1471.
42. Russell, B.J., et al., *Intestinal transgene delivery with native E. coli chassis allows persistent physiological changes.* Cell, 2022. **185**(17): p. 3263-3277 e15.
43. Zhu, Z., et al., *Lactate Mediates the Bone Anabolic Effect of High-Intensity Interval Training by Inducing Osteoblast Differentiation.* JBJS, 2023. **105**(5): p. 369-379.
44. Li, X., et al., *Lactate metabolism in human health and disease.* Signal Transduction and Targeted Therapy, 2022. **7**(1): p. 305.
45. Wallace, D.C., *A Mitochondrial Paradigm of Metabolic and Degenerative Diseases, Aging, and Cancer: A Dawn for Evolutionary Medicine.* Annual Review of Genetics, 2005. **39**(1): p. 359-407.
46. Murphy, K.F., G. Balázsi, and J.J. Collins, *Combinatorial promoter design for engineering noisy gene expression.* Proceedings of the National Academy of Sciences, 2007. **104**(31): p. 12726-12731.
47. Chertoff, J., et al., *Lactate kinetics in sepsis and septic shock: a review of the literature and rationale for further research.* Journal of Intensive Care, 2015. **3**(1): p. 39.
48. Lefevre, M., et al., *Probiotic strain Bacillus subtilis CU1 stimulates immune system of elderly during common infectious disease period: a randomized, double-blind placebo-controlled study.* Immunity & Ageing, 2015. **12**(1): p. 24.
49. Chai, Y., R. Kolter, and R. Losick, *A Widely Conserved Gene Cluster Required for Lactate Utilization in Bacillus subtilis and Its Involvement in Biofilm Formation.* Journal of Bacteriology, 2009. **191**(8): p. 2423-2430.
50. Ramirez-Peralta, A., et al., *Effects of Sporulation Conditions on the Germination and Germination Protein Levels of Bacillus subtilis Spores.* Applied and Environmental Microbiology, 2012. **78**(8): p. 2689-2697.